Direct Observation of Sub-Picosecond Equilibration of Excitation Energy in the Light-Harvesting Antenna of *Rhodospirillum rubrum*

H. Matthieu Visser,* Oscar J. G. Somsen,* Frank van Mourik,* Su Lin,‡ Ivo H. M. van Stokkum,* and Rienk van Grondelle*

*Department of Physics and Astronomy, Vrije Universiteit and Institute for Molecular and Biological Sciences, 1081 HV Amsterdam, the Netherlands; and ‡Department of Chemistry and Biochemistry and Center for Study of Early Events in Photosynthesis, Arizona State University, Tempe, Arizona 85287 USA

ABSTRACT Excitation energy transfer in the light-harvesting antenna of *Rhodospirillum rubrum* was studied at room temperature using sub-picosecond transient absorption measurements. Upon excitation of *Rs. rubrum* membranes with a 200 fs, 600 nm laser flash in the Q_x transition of the bacteriochlorophyll-*a* (BChl-*a*) absorption, the induced transient absorption changes in the Q_y region were monitored. In *Rs. rubrum* membranes the observed ΔOD spectrum exhibits ground state bleaching, excited state absorption and stimulated emission. Fast $Q_x \rightarrow Q_y$ relaxation occurs in ~100–200 fs as reflected by the building up of stimulated emission. An important observation is that the zero-crossing of the transient difference absorption (ΔOD) spectrum exhibits a dynamic redshift from 863 to 875 nm that can be described with by a single exponential with 325 fs time constant. The shape of the transient difference spectrum observed in a purified subunit of the core light-harvesting antenna, B820, consisting of only a single interacting pair of BChl-*a*s, is similar to the spectrum observed in *Rs. rubrum* membranes and clearly different from the spectrum of BChl-*a* in a protein/detergent mixture. In the B820 and monomeric BChl-*a* preparations the 100–200 fs $Q_x \rightarrow Q_y$ relaxation is still observed, but the dynamic redshift of the ΔOD spectrum is absent. The spectral kinetics observed in the *Rs. rubrum* membranes are interpreted in terms of the dynamics of excitation equilibration among the antenna subunits that constitute the inhomogeneously broadened antenna. A simulation of this process using a set of reasonable physical parameters is consistent with an average hopping time in the core light harvesting of 220–270 fs, resulting in an average single-site excitation lifetime of 50–70 fs. The observed rate of this equilibration process is in reasonable agreement with earlier estimations for the hopping time from more indirect measurements. The implications of the findings for the process of excitation trapping by reaction centers will be discussed.

INTRODUCTION

In photosynthesis, solar energy is converted into chemical free energy in the form of carbohydrates. In the last 15 years remarkable progress has been made in the understanding of the physical-chemical processes in photosynthesis. X-ray crystallography and other techniques have revealed the structure of several important pigment protein complexes, such as the bacteriochlorophyll-*a* (BChl-*a*) light-harvesting complex of the green sulphur bacterium *Prostecochloris aestuarii* (Matthews, 1979), the reaction center (RC) of the photosynthetic bacteria *Rhodopseudomonas* (*Rps.*) *viridis* (Deisenhofer et al., 1984) and *Rhodobacter* (*Rb.*) *sphaeroides* (Allen et al., 1987) and recently the major light-harvesting complex (LHC) of plants, LHC-II (Kühlbrandt et al., 1994). Very recently, the structure of the peripheral light-harvesting antenna (LH2) of *Rps. acidophila* was published (McDermott et al., 1995). In all these systems, interacting (bacterio-)chlorophyll molecules are positioned at center-to-center distances of 0.8–2.0 nm, allowing for fast excitation energy transfer and, in the case of RCs, fast electron transfer.

After the absorption of a photon by a pigment molecule from an antenna complex, the energy is rapidly transferred among the various pigments, either located within the same pigment-protein complex or on neighboring complexes. The rate at which the energy transfer process occurs depends on the distance between the antenna pigments involved and their relative orientation and spectral overlap (Förster, 1965). Earlier estimates based on the analysis of singlet-singlet annihilation experiments at room temperature in the light-harvesting antenna of photosynthetic purple bacteria arrived at hopping times of 0.5–1.0 ps (Den Hollander et al., 1983; Bakker et al., 1983; Deinum et al., 1989), resulting in single-site excitation lifetimes of 125–250 fs. Similarly, Owens et al. (1987) estimated single-step hopping times of 0.2 ps in the light-harvesting core-antenna of photosystem 1 (PS1) based on an analysis of the observed excitation trapping time as a function of the core-antenna size. Later results from picosecond absorption and fluorescence experiments were consistent with the idea of sub-picosecond hopping times (see for reviews Holzwarth, 1991; Sundström and Van Grondelle, 1991; and Van Grondelle et al., 1994), although in many cases slower phases in the equilibration process were also observed (Sundström et al., 1986; Freiberg et al., 1987; Holzwarth, 1991). Lowering the temperature from ambient to cryogenic temperatures results in increasingly unidirectional energy transfer from molecules absorbing at higher energy to molecules absorbing at lower energy and the appearance of wavelength dependent phases

Received for publication 11 October 1994 and in final form 25 May 1995.

Address reprint requests to Matthieu Visser, Department of Physics and Astronomy, Vrije Universiteit Amsterdam, De Boelelaan 1081, 1081 HV Amsterdam. Tel.: 31-20-444-7942; Fax: 31-20-444-7899; E-mail: matthieu@nat.vu.nl.

0006-3495/95/09/1083/17 $2.00

in the excitation equilibration kinetics characteristic for energy transfer in spectrally inhomogeneous systems (e.g., Freiberg et al., 1987; Pullerits et al., 1994b; Pullerits and Freiberg, 1992; Somsen et al., 1994).

The developments in ultrafast laser spectroscopy have made it possible to study the molecular mechanisms of photosynthetic excitation and electron transport in the early time (>50 fs) domain. With laser pulses as short as 100 fs, energy transfer times from ~100 fs to several tens of ps have been observed experimentally in plant and bacterial antenna systems. For instance, in the LHC-II of green plants a time constant of 0.5 ps for Chl-*b* to Chl-*a* transfer was observed (Eads et al., 1989); from fluorescence depolarization studies a time of ~0.2–0.3 ps was estimated for Chl-*a* → Chl-*a* transfer in LHC-II (Du et al., 1994) and PS1 (Du et al., 1993), times of 0.3–0.7 ps for energy transfer from B800 to B850 in the LH2 of a variety of photosynthetic purple bacteria (Trautman et al., 1990; Hess et al., 1994). In the latter case the B800 → B850 energy transfer was found to be weakly temperature dependent, the rate slowing down to 2.2–2.4 ps at 4 K. The latter rate was consistent with hole-burning results for the same system (Van der Laan et al., 1990; Reddy et al., 1991).

From energy-selective spectroscopic experiments and hole-burning data, it has been firmly established that the absorption bands of photosynthetic pigments in a protein environment are inhomogeneously broadened because of small variations in the local protein environment (Freiberg et al., 1987; Reddy et al., 1992a; Völker, 1989; van Mourik et al., 1993; Visschers, 1993b). The influence of inhomogeneous broadening on the process of excitation energy transfer in bacterial light-harvesting systems is currently under theoretical (Jean et al., 1989; Somsen et al., 1994; Trinkunas and Holzwarth, 1994) and experimental investigation, and for preparations at cryogenic temperatures a variety of specific effects have been described and explained in these terms. Examples are the multiexponential wavelength-dependent fluorescence and absorption decay (Timpmann and Freiberg, 1991; Van Grondelle et al., 1987), the increase in fluorescence polarization, and the shift of the emission maximum upon scanning the excitation wavelength to the low-energy part of the spectrum (Kramer et al., 1984; Van Mourik et al., 1992b; Gobets et al., 1994). The temperature dependence of the quantum yield of trapping as observed by Rijgersberg et al. (1980) may also be explained using inhomogeneous broadening. However, concerning the effects of inhomogeneous broadening on the kinetics of excitation energy transfer and trapping at room temperature, very little is known.

Whereas the structure of the RC of several photosynthetic purple bacteria has been resolved down to atomic resolution by x-ray diffraction, the structure of the light-harvesting antenna can only be deduced from spectroscopic data and transmission electron microscopy. From these data, it is indicated that the light-harvesting 1 antenna (LH1) has a ringlike structure. From spectroscopic data it was concluded that the Q_y transition dipole moments are oriented parallel to the membrane plane (Kramer et al., 1984). For *Rps. marina*, a diameter of 102 Å was found for a ringlike core light-harvesting antenna (LH1) surrounding the RC (Meckenstock et al., 1992). For *Rps. viridis*, a similar structure was reported earlier (e.g., Miller, 1982). In a recent study, a ringlike structure of six α,β-pairs for *Rb. sphaeroides* LH1 was suggested. The outer diameter would be 52 Å (Boonstra et al., 1993). It is often suggested that LH1 is structurally similar to LH2, for which several model structures were proposed (Pearlstein, 1991; Hunter et al., 1989). Simulations of energy transfer are usually performed on square lattices of connected subunits. We will discuss the consequences of these assumptions for our simulations in the Discussion section.

Over the past few years, we have intensively investigated a purified subunit of the LH1 antenna of photosynthetic bacteria, B820, consisting of an α,β-heterodimer and binding a single pair of BChl-*a* molecules (Miller et al., 1987; Visschers et al., 1991). The spectral properties of B820 (absorption spectrum and fluorescence upon narrow-band excitation at cryogenic temperatures) can be accounted for in terms of a model including excitonic interactions between the BChl-*a*s and energetic disorder (Van Mourik, 1993; Visschers et al., 1993b; Koolhaas et al., 1994; Pullerits et al., 1994a). The 820 nm transition of B820 was shown to be due to the allowed low-energy transition of the dimer. From the high steady state emission anisotropy of 0.35 it was concluded that dimer-to-dimer energy transfer was absent. It was shown that the B820 BChl-*a* dimer was the building block of the LH1 antenna of photosynthetic purple bacteria (Van Mourik et al., 1992a).

We have studied the early-time excitation energy transfer processes within the LH1 antenna of the photosynthetic bacterium *Rhodospirillum* (*Rs.*) *rubrum*. This antenna is characterized by a single absorption band at 880 nm. It has been estimated that 24 antenna BChl-*a* molecules per RC are present (Aagard and Sistrom, 1972). This size of the LH1 (core) antenna is generally found to be independent of growth (light) conditions. The antenna molecules function as a kind of "lake": 10–20 RCs are connected by energy transfer within a so-called domain (Den Hollander et al., 1983). From ps pump-probe and fluorescence measurements, it was found that antenna excitations decay in ~50 ps if the RC is in the open state (PIQ) and 200 ps in the closed state (P^+IQ^-) (e.g., Sundström and van Grondelle, 1991). With closed RCs also a faster, 30–50 ps component was found, which was ascribed to transfer processes from higher to lower energy pigments (Van Grondelle et al., 1987). From the low value of the observed initial polarization of the absorption changes it was concluded that a sub-ps equilibration process preceeded the trapping and slow equilibration phases (Sundström et al. 1986; Van Grondelle et al. 1987). Fast kinetics around the isosbestic point also seem to indicate such fast energy transfer (e.g., Van Grondelle et al., 1987). From singlet-singlet (S-S) annihilation measurements, hopping times of about 0.5–1 ps were extracted (Den Hollander et al., 1983; Bakker et al.,

1983; Deinum et al., 1989). In contrast, from model simulations (Pullerits and Freiberg, 1992) of the fluorescence and absorption kinetics observed in *Rs. rubrum* for temperatures from 4 to 300 K, a much slower hopping time of about ~60 ps was estimated. From more recent modeling of both fluorescence and transient absorption data taken at 77 K, a hopping time of ~15 ps was estimated (Pullerits et al., 1994b). In these models the transfer of excitation energy from LH1 to the special pair P of the RC was assumed to be slow. This was recently confirmed by direct time-resolved measurements on RC-LH1 systems of *Rb. sphaeroides* in which the rate of charge separation was selectively modified (Beekman et al., 1994). Another time-resolved study (Timpmann et al., 1993), in which the back-transfer from the RC to the antenna was measured, came to the same conclusion.

In this work, a comparison of the sub-ps time-resolved spectra of membranes of *Rs. rubrum* with isolated dimeric antenna subunits (B820) and monomeric BChl-*a* in a protein-detergent mixture is made. We conclude that the dominant phase in spectral equilibration at room temperature occurs in about 300 fs, and is due to energy transfer within the inhomogeneously broadened LH1 antenna. Additional slower components, as observed in a variety of other photosynthetic systems, cannot be detected. To analyze our data, we employ a simple theoretical model, using Förster energy transfer in an inhomogeneously broadened LH1 antenna. On the basis of this model, we argue that sub-100 fs phases in the equilibration, which are beyond the time resolution of our experiment, are expected to be substantially smaller than the 300 fs phase that was detected. We will discuss the implications of our observations for excitation energy transfer within the LH1 antenna and for transfer from the antenna to the RC.

MATERIALS AND METHODS

Rs. rubrum cells were grown and chromatophores isolated from these as described, e.g., in Visschers et al. (1993a). B820 particles were prepared from the carotenoid-less mutant of *Rs. rubrum* G9 as described in Miller et al. (1987). To obtain BChl-*a* in protein detergent, an additional amount of *n*-octyl-β-D-glucopyranoside (OG) was added to the B820, so that the total amount of OG corresponds to 2% w/v. At these detergent concentrations, one obtains an absorption band at 777 nm, corresponding to absorption of monomeric BChl-*a*, as described in Visschers et al. (1991). In all cases, the concentration of the sample was chosen so that in the spinning cell with 1.7 mm path length, the optical density (OD) was 1.2 at the peak of the absorption in the Q_y band corresponding to an OD of about 0.1 at the excitation wavelength in the Q_x absorption band. The low OD at the excitation wavelength assures that front and back regions of the sample receive almost the same excitation density.

Sub-ps spectral changes were measured by using a sub-ps spectrophotometer similar to the one described by, e.g., Taguchi et al. (1992). A sync-pumped double dye-jet laser (model 774 from Coherent, Palo Alto, CA) provides pulses of 320 fs full width at half maximum (FWHM) autocorrelation, corresponding to a 200 fs pulse duration assuming a squared hyperbolic secant auto correlation. These pulses were amplified in a three-stage dye amplifier pumped at 30 Hz by a regenerative amplifier (RGA from Continuum). Pulses could be tuned from 595 to 610 nm, using rhodamine 6g (R6G) 3,3′-diethyloxacarbo cyanine iodide (DODCI) as gain and absorber media, respectively, in the dye laser, and sulforhodamine dissolved in water in the dye amplifier. White light, generated in water by means of continuum generation, was split in a reference and a probe beam that were imaged by means of an imaging monochromator on two separate diode arrays (512 pixels each) that were read out single shot at 30 Hz. In the probe beam, group velocity dispersion is compensated by means of two SF10 prisms placed at 38 cm distance. Pump and probe were overlapped in the sample. The pump beam was polarized at magic angle (57.4°) with respect to the probe beam in all measurements. Samples were contained in a spinning cell (so that sample flow speed was 10 m/s) and placed slightly before the focus of the pump beam. Here the diameter of the pump spot was ~2 mm, and the probe and reference spot had ~1 mm diameters. The energy of the pump pulse at the sample was maximally 7 μJ, and was reduced by means of neutral density filters to 1 μJ typically. In some experiments on the B820 preparation, 600 nm laser pulses for excitation of the sample were obtained using a 5 nm FWHM, 1 mm thin interference filter to select a part of a continuum. This light was subsequently amplified to a few μJ energy. The instrument response for all detection wavelengths simultaneously was obtained by measuring the induced birefringence in CS_2 (Greene and Farrow, 1983; see also Fleming, 1986). After proper group velocity dispersion compensation, this signal rose from 10 to 90% in 400 fs typically at all wavelengths. The signal at the central detection wavelength reached its maximum less than 100 fs earlier than the outer wavelengths, 65 nm from the center wavelength. During data collection, 780 laser shots were averaged per time point. A scan of some 20 time points was made, from early to late times. Typically, five of these scans were taken and averaged. It was checked that the baseline (signal before $t = 0$) had not changed after the scan, and that the signal in the next scan had not changed within signal to noise. Absorption spectra of the sample were taken before and after the measurement, and were found to be identical.

RESULTS

In the experiments reported in this paper, membranes of *Rs. rubrum*, B820-complexes and BChl-*a* in detergent were excited in the Q_x region and the induced absorption/stimulated emission (ΔOD) of each sample was measured at specified time intervals after excitation. Fig. 1 shows the ΔOD spectra at various delay times in the wavelength region from 820 to 945 nm, obtained after excitation of *Rs. rubrum* membranes with a 1.2 μJ laser flash at 600 nm. The inset shows the absorption spectrum of the sample with an indication of the excitation and detection wavelengths. The excitation corresponds to ~1 excited dimeric subunit per 12 subunits if one assumes ground state bleaching and stimulated emission to contribute to the signal to the same amount. We define time $t = 0$ to coincide with the moment of measurement of the ΔOD spectrum indicated as spectrum 1. From the time evolution shown in Fig. 1, it is clear that the ΔOD grows in in about 400 fs (10 → 90% signal). The minimum in the ΔOD spectrum near 893 nm corresponds to a bleaching of the major Q_y transition of LH1. The observed response time is in agreement with the rise time of the transmission changes observed in CS_2 due to induced birefringence. Apart from the in-growth several important aspects of the ΔOD spectra shown in Fig. 1 should be noted. In the first place we point to the fact that in the very early time the ΔOD spectrum (Fig. 1, spectrum 3, measured after 333 fs) shows induced absorption in the wavelength region above $\lambda = 920$ nm. At later times the sign of the signal in this wavelength region has reversed and the ΔOD spectrum is characteristic for stimulated emission. The width

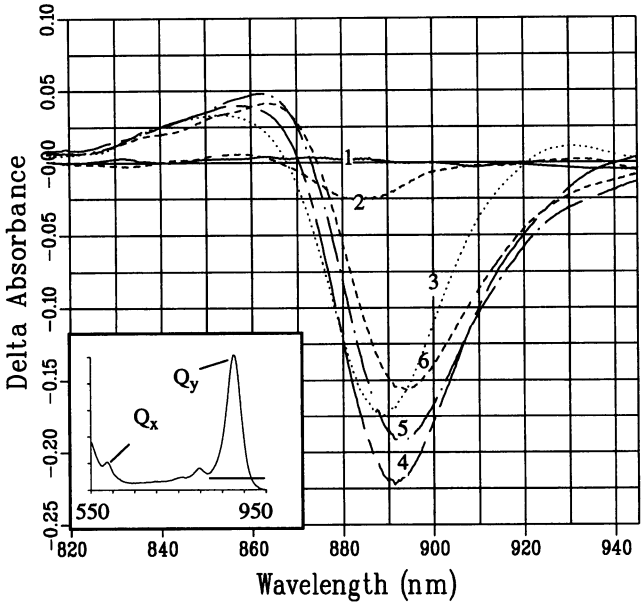

FIGURE 1 Observed difference spectra with different time delays between the 600 nm excitation and the probe pulse. (*Spectra 1–4*) 0, 166, 333, and 500 fs. (*Spectrum 5*) 1.0 ps. (*Spectrum 6*) 2.0 ps. The inset shows the absorption spectrum of the sample from 550 to 950 nm; the horizontal bar indicates the detection range of the measurements. Between 2 and 10 ps, the signal decayed because of S-S annihilation. In this time interval, the observed difference spectra did not show any further changes in shape or position (data not shown).

(FWHM) of the ΔOD spectrum increases from 20.7 nm in number (no.) 2, 25.0 nm in no. 3, 30.0 nm in no. 4, to 30.2 nm in no. 5 and later spectra. This buildup of stimulated emission reflects the $Q_x \rightarrow Q_y$ relaxation, and we estimate a time constant for this process of 100–200 fs, consistent with estimates in other related systems (Du et al., 1992). (We will come back to this point below). A second and important feature of the set of spectra shown in Fig. 1 is that the ΔOD spectrum shifts as a function of time; the isosbestic point of spectrum 2 is at 863 nm and moves to 875 nm in spectrum 6, taken 1.8 ps later. The total shift amounts to 12 nm or 150 cm^{-1}. This shifting of the isosbestic point is a direct manifestation of spectral equilibration in the light-harvesting system, and below we will demonstrate that this phenomenon is due to ultrafast excitation-energy transfer. Finally, after the buildup of the bleaching, a distinct decay of the ΔOD spectrum with increasing delay time is observed which must be ascribed to bi-excitation annihilation, since it showed an excitation-energy dependent decay rate, in agreement with S-S annihilation theory (Den Hollander et al., 1983; Paillotin et al., 1979).

The bimodal shape of the spectra deserves some comments. Similar bimodal difference spectra have been reported upon excitation of a variety of photosynthetic systems (Nuijs et al., 1985; Lin et al., 1992). These difference spectra are very characteristic for aggregates of interacting pigments (see also Van Mourik et al., 1993). The spectra observed for $t > 0.5$ ps are in fact rather similar to those reported in the earlier work of Nuijs et al. (1985) on the same photosynthetic system. In this work, membranes were excited at 532 nm (in the carotenoid absorption band) using 35 ps pulses. Because of energy transfer from carotenoid to BChl-*a* with an estimated efficiency of 30%, the difference spectra in the 760–950 nm region are similar to the difference spectra in Fig. 1. These authors find the isosbestic point at 857 nm for a maximum bleaching (−ΔOD) of 0.25 and at 868 nm for a maximum bleaching of 0.05 in the "t = 0" spectra. The low-intensity result agrees reasonably well with the results with higher time resolution reported here. The spectra in Fig. 1 are part of a set extending from 0 to 10 ps. Spectra between 2 and 10 ps were found identical in shape and position, but the strength decreased rapidly due to S-S annihilation.

In Fig. 2, the shift of the zero-crossing of the spectra presented in Fig. 1 is shown as a function of delay time (Fig. 2, *open squares*). Also a few points obtained from spectra recorded with a 4× lower bleaching signal have been added (Fig. 2, *open circles*). The data points are fitted to a single exponential with 325 fs time constant, and we conclude that these 325 fs kinetics describe the time dependence of the isosbestic point reasonably well. In addition, the shift kinetics are independent of the excitation density (within the applied range of energies). The low excitation density dataset (not shown) extended up to 30 ps; between 2 and 30 ps the spectra did not exhibit any further shifting or changing shape.

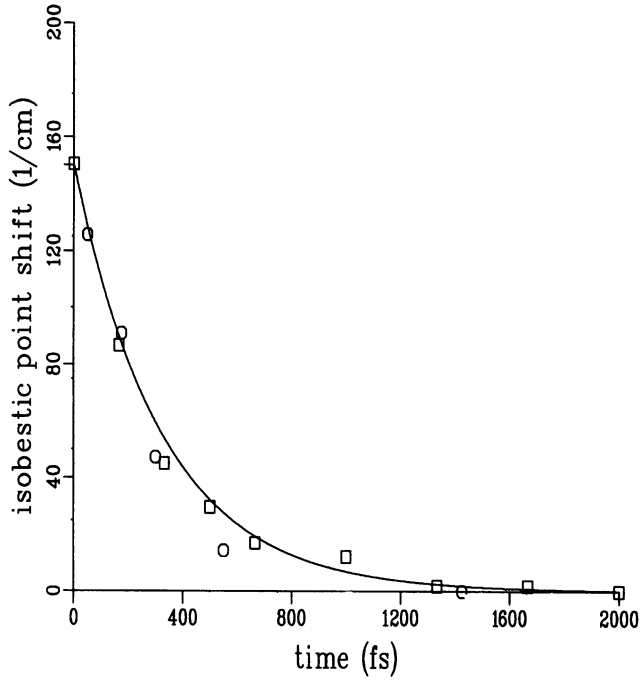

FIGURE 2 The shift of the isosbestic point (in cm^{-1}) as a function of time, fitted with a single exponential with 325 fs time constant. Datapoints from a set including Fig. 1 (□) and from a set measured with 4 times lower excitation density (○).

Fig. 3 shows the results of a similar set of experiments on the B820 complex, the isolated antenna subunit of LH1 of *Rs. rubrum*. Again, the signal grows in with the instrument response, which was ~500 fs FWHM in this experiment but, in contrast to the results shown in Fig. 1, no significant shift of the zero-crossing point in the ΔOD spectra is observed. From the complete dataset from which the spectra in Fig. 3 are taken, we estimate that a maximal shift of 3 nm could be hidden in the noise on the data. Two conclusions can be drawn from these results. 1) The shift kinetics observed in LH1 do not reflect relaxation of the excited BChl-*a* dimer within the protein surroundings, since that process should also occur in B820. 2) Since the 820 nm band of B820 is due to the lower exciton component of a dimer of BChl-*a*, and coupling between dimers is absent (Visschers et. al, 1993b), the 325 fs zero-crossing shift observed for *Rs. rubrum* membranes must reflect the excitation energy transfer dynamics. In a separate experiment (not shown) we checked that the amplitude of the B820 ΔOD spectrum did not change during the first 40 ps after excitation, consistent with the 0.72 ns excited state lifetime determined in a time-correlated single photon-counting experiment (Chang et al., 1990), and confirming the absence of energy transfer and bi-excitation annihilation in B820 (Van Mourik et al., 1991). It should be noted that the B820 excited state difference spectrum is again bimodal and very similar in shape to the signal obtained from intact *Rs. rubrum* membranes. Because of the absence of excitation energy transfer and bi-excitation annihilation in B820, it is likely that the observed broadening of the B820 difference spectrum after 600 nm excitation arises from $Q_x \rightarrow Q_y$ relaxation. We analyzed the B820 difference spectra during the first ps after Q_x excitation using global analysis (see, e.g., Van Stokkum et al., 1994). For this analysis, a dataset obtained using slightly shorter excitation pulses than in the dataset of Fig. 3 was used. The data were fitted to a scheme in which every excitation creates a difference spectrum due to the Q_x excited state, which decays with a time constant τ_{ic} into a difference spectrum due the Q_y excited state. The results of this scheme were convoluted with a Gaussian instrument response with Γ_{instr} FWHM width. Free parameters here were τ_{ic}, the Q_x and Q_y excited state difference spectra and the width of the instrument response Γ_{instr}. The best fit was found for τ_{ic} = 160 fs, Q_x and Q_y excited state difference spectra as shown by the solid lines in Fig. 4, *a* and *b*, respectively, and Γ_{instr} = 230 fs. The root-mean-square (rms) value of the residuals of this fit was equal to 1.6% of the maximum bleaching signal. The Q_x and Q_y excited state difference spectra were decomposed into ground state bleaching, excited state absorption, and stimulated emission as follows. Both spectra contain the same amount of ground state bleaching, which was assumed to have the shape of the ground state absorption spectrum, since excitation was nonselective. The Q_x excited state was not expected to have any stimulated emission in the wavelength region of detection. The stimulated emission from the Q_y excited state was modeled by the room-temperature emission spectrum of B820 measured with 600 nm broadband excitation. Assuming no further (sub-) ps dynamics, we put the strength of the stimulated emission in the Q_y excited state difference spectrum equal to the ground state bleaching contribution. The Q_x and Q_y excited state absorption spectra were modeled as the sum of two skewed Gaussians (see, e.g., Sevilla et al., 1989). This results in an

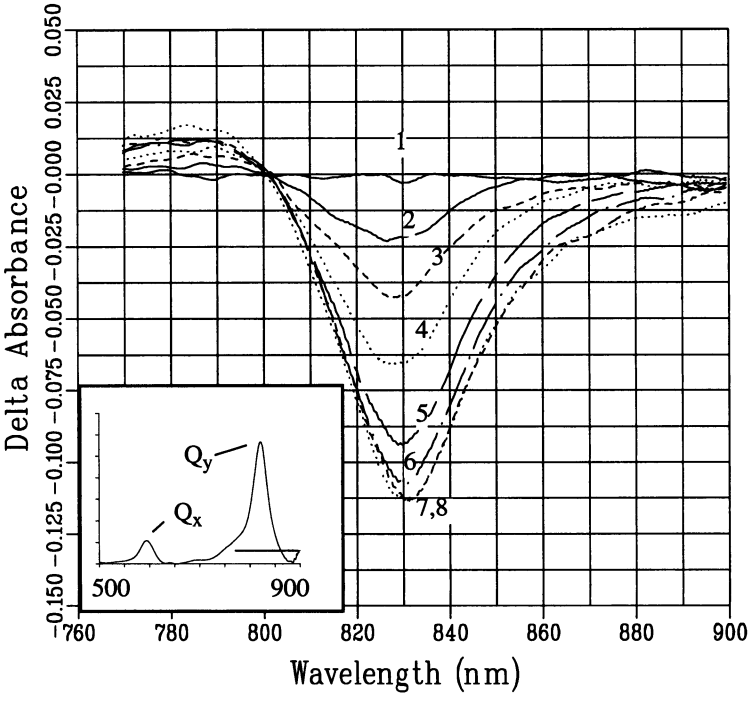

FIGURE 3 Difference spectra obtained upon 600 nm Q_x excitation of B820 antenna subunits at 600 nm. Shown is the in-growth of the signal. Spectra were taken at t = −300, 100, 233, 267, 500, 633, and 767 fs; and 7.4 ps (·····), respectively. Compared with Fig. 1, it is striking that the isosbestic point hardly shifts as a function of time. As in Fig. 1, the inset shows the absorption spectrum of the sample, with indication of the Q_x and Q_y absorption bands, as well as the region of the detection wavelengths (*horizontal bar*).

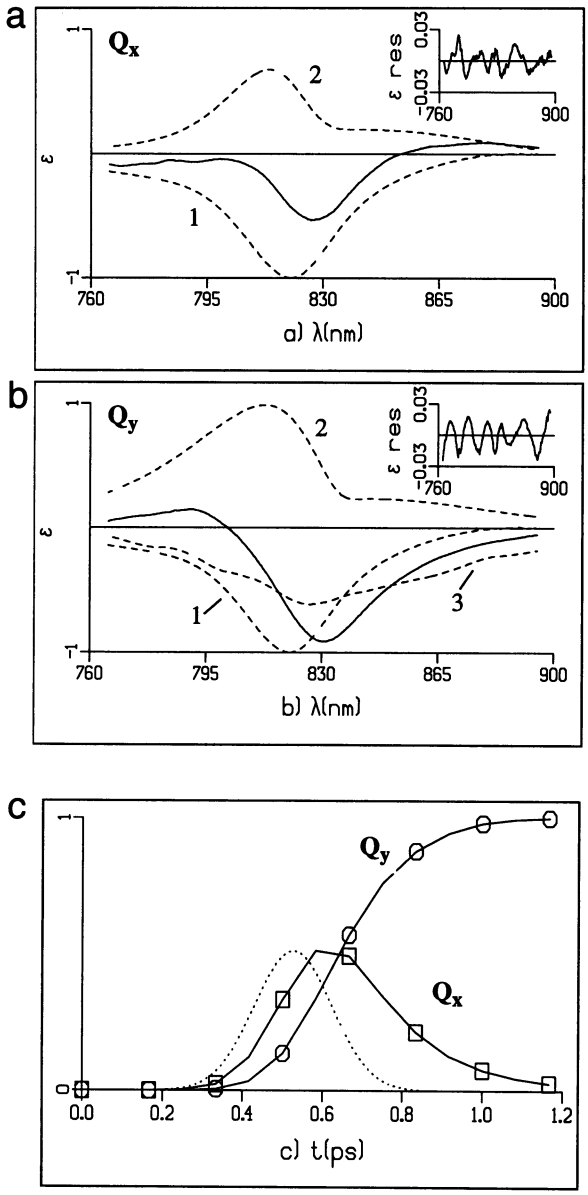

FIGURE 4 Difference spectra obtained from a global analysis of the B820 difference spectra during the first ps after Q_x excitation. A sequential model, in which the Q_x excited state decays with time constant τ_{ic} into the Q_y excited state, was fitted to the data. For the Q_x excited state, this resulted in a difference spectrum as in *a*. This spectrum is decomposed into ground state bleaching (fitted with the ground state absorption spectrum) and excited state absorption as shown. The Q_y excited state gives rise to a difference spectrum with the same amount of ground state bleaching. In addition, we put the strength of the stimulated emission equal to the ground state bleaching. The stimulated emission was modeled by the steady state fluorescence spectrum, measured with broadband excitation at 600 nm. This then results in a decomposition, as in *b*. The ground state bleaching contribution is indicated by *1*, the excited state absorption spectrum by *2*, and the stimulated emission by *3*. From the fit, a time constant τ_{ic} of 160 fs is found for the $Q_x \rightarrow Q_y$ relaxation. (*c*) shows the populations of the Q_x and Q_y excited states as a function of time in the fit of the sequential scheme to the transient absorption data. The instrument response as estimated from the fit is indicated with the dotted line. See text for details.

optimal decomposition as shown. It is evident that the Q_y excited state absorption spectrum is significantly stronger than the Q_x excited state absorption spectrum. The strength of the Q_y excited state absorption spectrum is almost equal to the ground state absorption, but peaks at a shorter wavelength, 813 nm. Residuals for the Q_x and Q_y difference spectra are shown in Fig. 4 (*insets*, *a* and *b*). These residuals are the difference between the difference spectrum obtained from the global analysis and the decomposition. For the Q_x spectrum, the rms value of these residuals is 8.6×10^{-3}; for the Q_y spectrum it is 1.2×10^{-2}. These can be compared with the strength of the ground state contribution with a minimum of -1 in both spectra.

Fig. 4 *c* shows the populations of the Q_x and Q_y excited states as a function of time in the fit of the sequential scheme to the transient absorption data.

Fig. 5, *a–c*, compares the ΔOD spectra measured at 0.8 ps (after the in-growth of the signal) of B777, (the dissociated B820 complex, Fig. 5 *a*), the purified B820 complex of *Rs. rubrum* (Fig. 5 *b*) and of membranes of *Rs. rubrum* (Fig. 5 *c*). For comparison, the steady state absorption spectra of the preparations in the same wavelength region are shown as well. It is clear that the ΔOD spectrum of the B777 monomer, when decomposed in ground state bleaching and stimulated emission, has a rather flat and weak excited state absorption spectrum, unlike B820 and the intact membranes. Such a flat and weak (compared with the $S_0 \rightarrow S_1$ ground state absorption) excited state spectrum was extracted from sub-ps pump-probe spectroscopy data on BChl-*a* in organic solvents (Becker et al., 1991) as well. The ΔOD spectra of B820 and the membranes both exhibit strong excited state absorption on the high energy side of the original absorption band. This is characteristic for an excited dimer (or larger aggregate) of interacting BChl-*a* molecules, in which most of the ground state absorption is concentrated in the lowest energy exciton state, because of a "head-to-tail orientation" (dipole moments on one line) of the Q_y transition dipole moments (Van Mourik et al., 1991). Note that the "777" monomeric BChl-*a* spectra are substantially wider than the B820 and LH1 spectra, as is expected from the excitonic nature of B820 of LH1. The widths (FWHM) of the absorption spectra at room temperature are 1244, 565 and 516 cm^{-1} for the 777, B820 and LH1 antenna preparations respectively. Part of this difference could arise from exchange narrowing in B820 and LH1 (Knapp, 1984).

DISCUSSION

In this work we show that in membranes of *Rs. rubrum* a dynamic process is observed, the shifting of the zero-crossing point with a major kinetic component of 325 fs. This phenomenon is characteristic for spectral equilibration due to rapid excitation energy transfer in a spectrally inhomogeneous system. The major experimental reason for ascribing this phenomenon to excitation energy transfer is that it

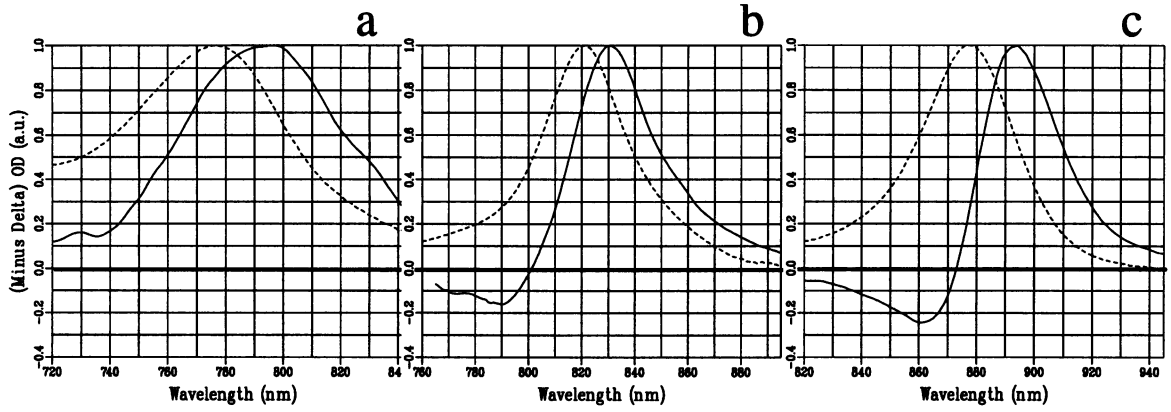

FIGURE 5 Difference spectra (——) shortly after the in-growth of the signal (t = 800 fs) for three preparations. (*a*) Monomeric BChl-*a* in protein detergent obtained by dissociating B820 dimeric subunits by means of a 2% w/v OG concentration. (*b*) B820 dimeric subunits. (*c*) *Rs. rubrum* membranes. In all cases, the absorption spectrum of the preparation in the same wavelength region is shown as well (- - -).

is not observed in the B820 subunit of LH1, which is a protein-bound BChl-*a* dimer. Within the experimental limits, the excitation equilibration dynamics, as reflected by the shift kinetics, are independent of the excitation density and are not affected by bi-excitonic annihilation kinetics. This conclusion is further supported by experiments performed by Xiao et al. (1994), who observed a similar dynamic shift in the transient absorption spectrum in an LH1-RC mutant of *Rb. capsulatus* with relatively low excitation density (a maximum bleaching of 0.04). Below we will first discuss the other dynamic process observed in this work, the $Q_x \rightarrow Q_y$ relaxation and the spectral changes associated with this process. Then we will summarize our conclusions concerning the excitation equilibration dynamics, and show that a simulation of the excitation energy transfer process based on reasonable physical parameters is consistent with the obtained results. Finally we will compare our results with experiments in other photosynthetic systems.

Spectral changes due to $Q_x \rightarrow Q_y$ relaxation

The analysis in Fig. 4 indicates that $Q_x \rightarrow Q_y$ relaxation is visible in our data as a changing of shape of the difference spectrum of B820 during the first ps after Q_x excitation. Upon comparing the difference spectra due to the Q_x and Q_y excited state, it appears that the Q_y spectrum is more intense. This can reasonably well be attributed to stimulated emission, as is obvious from the decomposition. Both states appear to have a peak in the excited state absorption spectrum at the blue side of the B820 ground state absorption spectrum, at 814 and 813 nm, respectively. The Q_y excited state absorption spectrum has almost the same strength (amplitude of 0.99) as the ground state absorption and agrees well with the spectrum expected for a BChl-*a* dimer with $\geq$90% of the dipole strength in the low-energy exciton band (calculation not shown). It should be mentioned that, because of the small Stokes' shift, the decomposition of the kinetic spectra into ground state bleaching, excited state absorption, and stimulated emission is not unique, unless the additional assumption is made that stimulated emission and ground state bleaching contribute equally to the Q_y excited state difference spectrum. This assumption, however, does not influence the value of τ_{ic}, since the decomposition was done after the sequential model was fitted to the data. Since the value for the instrument response estimated from the global analysis is somewhat short (230 fs), we also performed a fit with larger (fixed) values for the instrument response. Fixing Γ_{instr} at 286 fs resulted in a fit with 3% larger rms error; however, the estimated time constant τ_{ic} then was 87 fs. The difference spectra due to the Q_x and Q_y excited state were influenced to a minor extent. We therefore conclude that the difference spectra as in Fig. 4, *a* and *b* represent the difference spectra due the to Q_x and Q_y excited state reasonably well, but that we can only approximate the time constant for $Q_x \rightarrow Q_y$ relaxation to be close to 100–200 fs. This approximated time constant is in reasonable agreement with the number suggested for the $Q_x \rightarrow Q_y$ relaxation within the special pair in isolated RCs (Du et al., 1992). We note that this relaxation time between electronic states is quite similar to that observed for other, non-protein bound chromophores (Shreve et al., 1991). The early-time spectral changes (specifically: the broadening of the bleaching spectrum) observed in membranes of *Rs. rubrum* show that the $Q_x \rightarrow Q_y$ relaxation process is also present. Although the fast shifting of the isosbestic point does not allow an accurate estimate of the associated time constant, we estimate it to be similar.

The dynamic redshift

We ascribe the rapid shifting toward lower energy of the transient ΔOD spectra in membranes of *Rs. rubrum* to fast energy transfer within the inhomogeneously broadened LH1, during which the excitation density equilibrates over all the spectral forms within the inhomogeneous distribution. The similarity of the ΔOD spectra of B820 and those of the intact

membrane of *Rs. rubrum* is striking (apart from the ~63 nm difference in position), and we consider this as one more reason to view the *Rs. rubrum* LH1 antenna as an aggregate of weakly interacting dimeric subunits. In this view, each dimer within the LH1 antenna occurs at a somewhat different energy, most likely because of small variations in the local protein surroundings of the constituting dimers (Van Mourik et al., 1993; Koolhaas et al., 1994; Pullerits et al., 1994a). The distribution of energies of the subunits is given by the so-called "inhomogeneous distribution function" (IDF). The absorption spectrum is given by a convolution of this IDF with the homogeneous absorption spectrum, i.e., the absorption spectrum associated with a single subunit. Rapid excitation energy transfer between subunits within the IDF, leading to a Boltzmann distribution over the subunits within the IDF ("thermalization"), is expected upon excitation to a non-equilibrium state of the LH1 antenna.

One can calculate the "excitation energy distribution," which gives the percentage of the excitations to be found at each energy, as a function of time. Immediately after homogeneous (i.e., nonselective) excitation it is equal to the IDF. After equilibration the population of the low-energy dimers has increased at the expense of the high-energy subunits and the product of the Bolzman factor e^{-E/k_BT} with the IDF gives the new distribution, which is shifted to lower energy. If each dimer would have an infinitely narrow absorption band, the transient bleaching would simply be equal to the distribution of the excited state energies, at all times. However, this is not the case; the relation is complicated by the presence of stimulated emission and excited state absorption. But, if we assume that all dynamics except for the equilibration are independent of the spectral shift of the dimer, each individual excited state will give rise to a ΔOD spectrum with the same shape but shifted depending on the energy the dimer occupies in the IDF. In that case the observed ΔOD spectrum is simply a convolution of this individual spectrum with the distribution of excited state energies. Furthermore, if this spectrum is sufficiently linear around the isosbestic point, the transient shift of the isosbestic point is equal to the shift of the average of this distribution.

The 325 fs time constant for the shifting of the ΔOD spectra in Fig. 1 is close to the instrument response. We performed simulations in which a monoexponentially shifting difference spectrum was convoluted with a Gaussian instrument response. It was shown that because of a 300 fs (FWHM) instrument response, 10–15% of a shift with 300 fs time constant can be washed out. For faster time constants, this number is larger. The observed 12 nm shift is therefore a lower limit, but it is accurate to 10–15% if no <100 fs time constants are present in the equilibration.

Dynamical simulations of energy transfer in inhomogeneous lattices to describe energy equilibration

The main parameters governing the excitation transfer dynamics within the LH1 antenna are the number (N) of connected subunits, the number of neighbors of each site (= the coordination number z), and their relative orientations and distances. The other parameters are the amount of energy disorder, reflected in the inhomogeneous bandwidth Γ_{IDF}, the absorption and emission of a single subunit, reflected in the width of a Gaussian absorption band, Γ_{hom}, the Stokes' shift S, and the temperature T. The magnitude of the transient shift of the excitation energy distribution depends only on three of the parameters mentioned above: N, Γ_{IDF}, and k_BT. Therefore we investigate this first. In the following we assume that the homogeneous spectra are time-independent. This is justified by the B820 experiment, which shows that any time dependence in the transient absorption spectrum is small.

If initially all subunits have an equal chance to be excited, then, after several energy transfer steps, the low-energy subunits will have a higher probability of being excited than do high-energy subunits. This probability is given by the Boltzmann distribution. The process of equilibration thus gives rise to a shift toward lower energy of the observed bleaching and stimulated emission spectra. We can quantify these considerations using the following assumptions. 1) The number of subunits in a domain is large in the sense that the inhomogeneous distribution observed in the absorption spectrum is also observed in every single domain. 2) Because of nonselective excitation, the initial spectrum consists of a bleaching of the whole IDF band. 3) The final state in every domain is described by a Boltzmann distribution over the subunits within the IDF. 4) The IDF can be described by a Gaussian. Then, the initial ΔOD spectrum is given by a convolution of the IDF and the "homogeneous ΔOD spectrum" (i.e., the difference spectrum associated with a single subunit in the Q_y excited state). The equilibrated spectrum is obtained simply by multiplying the IDF with the Boltzmann distribution factor e^{-E/k_BT}, resulting in a shifted IDF, which is again Gaussian with width Γ_{IDF}, but shifted toward lower energy by the amount in Eq. 1. Upon convoluting this shifted IDF with the homogeneous ΔOD spectrum, one obtains an equilibrated difference spectrum, corresponding to the spectrum measured after a few ps, which is shifted to lower energy by the same amount:

$$\text{shift} = \frac{\Gamma_{IDF}}{8 \ln 2} \cdot \frac{h\Gamma_{IDF}}{k_BT} \qquad (1)$$

Here, h is the Plank constant and k_B is the Boltzmann constant. We will define Γ values as FWHMs and (for Gaussians) σ values as rms widths. So $\Gamma = 2\sqrt{2 \ln 2} \cdot \sigma$. In Eq. 1, the unit for Γ_{IDF} is cm^{-1}, which we will convert to a width in nm. To explain the observed 12 nm shift would require a Γ_{IDF} of 32 nm according to this formula. Recently, the homogeneous line shape of the B820 antenna subunit was investigated (Pullerits et al., 1994a). To explain energy-selective fluorescence measurements, a wide (24 nm at 4 K, 27 nm FWHM at 295 K) homogeneous spectrum had to be assumed. Applying this value to the antenna, one calculates a width Γ_{IDF} of 30 nm FWHM to match the 40 nm FWHM

of the absorption spectrum. So our description yields reasonable results when realistic linewidths are inserted at room temperature. Note that Eq. 1 cannot be used for cryogenic temperatures: for $T \rightarrow 0$, the shift goes to infinity. The reason for this is that at low temperatures, excitations can be locally trapped, and a Boltzman equilibrium over a large domain cannot be reached, which was the first assumption in deriving Eq. 1.

If the number (N) of connected subunits is not so large, the equilibration may not be complete, and as a consequence the total shift of the distribution of the excitation energies will be less than predicted by Eq. 1. An obvious example of this is B820, where all subunits are disconnected ($N = 1$) and no equilibration is possible. For larger domains, one can take N subunits from an inhomogeneous distribution, impose a Bolzman distribution over these subunits, and calculate the average energy with respect to the center of the IDF. Fig. 6 shows the results of such an approach as a function of N for $\Gamma_{IDF} = 22$, 33 and 40 nm. As expected, the shift is larger for larger values of Γ_{IDF}. It can be seen that the shift converges to the value obtained in Eq. 1 for infinitely large systems, and that this limit is almost reached when $N = 25$.

From previous experiments it was concluded that 500–1000 antenna subunits are connected by means of excitation energy transfer (Den Hollander et al., 1983; Bakker et al., 1983; Deinum et al., 1989). To reach the lowest subunit in such a large domain would therefore take >30 hops on the average, and on first sight one would expect that the shift of the difference spectrum would continue on longer time scales. As mentioned, from $t = 2$ to $t = 50$ ps we do not observe any further shift. However, as we can see from the results of Fig. 6, thermal equilibration over only 25 subunits already results in a distribution close to the thermal distribution in an infinite system for a reasonable value of Γ_{IDF}. Therefore, even though maybe as many as 500–1000 subunits are connected by energy transfer the spectral equilibration can be nearly complete in less than 10 times the average hoptime. The simulations in the next section will support this consideration.

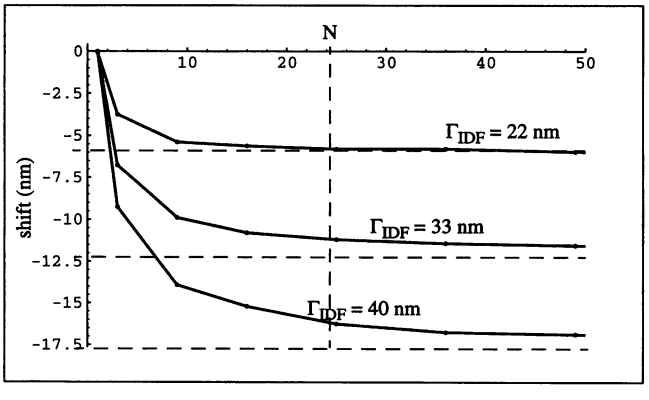

FIGURE 6 Equilibration shift of the average of the excitation energy distribution for systems with a finite number of subunits (N) for $\Gamma_{IDF} = 22$, 33, and 40 nm ($\kappa = 1.4$, 0.7, and 0 respectively). Calculations were done for $T = 300$ K, which corresponds to $k_BT = 16$ nm in the LH1 absorption band (at 880 nm). It is obvious that the thermal distribution over 25 subunits closely resembles the thermal distribution over an infinitely large number of connected subunit (- - - - -) for $\Gamma_{IDF} = 33$ nm. As expected: for larger inhomogenous widths (larger Γ_{IDF}), a larger number of subunits in a system is needed to make the thermal distribution over the system similar to the distribution in an infinite system.

Finding a reasonable set of parameters

To investigate the kinetics of the observed shifting of the transient spectra in the membranes and its dependence on various parameters, we simulated the energy transfer process between subunits placed in a two-dimensional (2D) square lattice. A 2D structure best describes the photosynthetic membrane of purple bacteria. We will discuss other (than square) 2D lattices in the next section. As before, the homogeneous absorption and fluorescence bands were supposed to be Gaussian with identical width Γ_{hom} and a relative shift S; the energies were normally distributed with a width of Γ_{IDF}. Thus, the absorption spectrum, being the convolution of the homogenous absorption spectrum and the IDF, is also Gaussian, with width Γ_{tot}. It is easily seen that $\Gamma_{hom}^2 + \Gamma_{IDF}^2 = \Gamma_{tot}^2$. As was mentioned, one measures $\Gamma_{tot} = 40$ nm for LH1 at room temperature. The rate of energy transfer from a site with energy level E_1 to a neighboring site with energy level E_2, $W(E_1 - E_2)$, was calculated from Förster's overlap of the absorption band of the accepting site with the fluorescence of the donor:

$$W(E_1 - E_2) = \frac{1}{\tau_0} \exp\left[-\frac{1}{4}\left(\frac{E_1 - E_2 - S}{\sigma_{hom}}\right)^2\right] \qquad (2)$$

Here, τ_0 is a time scaling factor equal to the transfer rate with optimal spectral overlap. In the simulations, also transfer between subunits more than a single lattice distance apart was taken into account. Since Förster energy transfer shows a $1/R^6$ dependence, we found that for our simulations on LH1 at room temperature, energy transfer between nearest neighbors dominates the process. Eq. 2 has to obey detailed balance:

$$\frac{W(E_1 - E_2)}{W(E_2 - E_1)} = \exp\left(\frac{E_1 - E_2}{k_BT}\right) \qquad (3)$$

for all values of $E_1 - E_2$. This is possible only if:

$$\sigma_{hom}^2 = Sk_BT \qquad (4)$$

This means that one cannot choose all spectral parameters independently. We use σ_{hom} as an independent parameter and use Eq. 4 to calculate S. This opens the possibility for an independent check of our results. We use a 5×5 square lattice with periodic boundary conditions, mainly because we have seen from the above calculations that the size of the equilibration shift hardly changes for larger systems (Fig. 6). The energy of each subunit is chosen randomly according to the IDF. The transfer rates are calculated according to Eq. 1, the subunits are excited homogeneously, and the

development of the population of each subunit as a function of time is calculated numerically. From this, the average of the excitation energy distribution is evaluated as a function of time, and this is then further averaged over a number of systems (typically 10^4) until the standard deviation is <1%. To obtain time constants, the shift was then fitted with a one- or two-exponential decay:

$$\langle E\rangle(t) \equiv \sum_{i=1}^{1,2} A_i e^{-t/\tau_i} - A_0 \qquad (5)$$

Simulations were performed for several values of Γ_{hom}. Since the total bandwidth is a constant, it is useful to define $\kappa = \Gamma_{hom}/\Gamma_{IDF}$. Large values of κ, e.g., $\kappa > 2$, indicate that the absorption spectrum is mainly determined by the homogeneous bandwidth. In this case the transfer time between any two neighboring subunits is almost equal to τ_0. On the other hand, small values, e.g., $\kappa < \frac{1}{2}$, indicate that inhomogeneous broadening determines the observed absorption profile. Since the energy transfer rate is very sensitive for the energy gap between two neighboring subunits, a wide range of subunit-subunit transfer rates occurs in that case. This slows down the equilibration. However, the approximation of the homogeneous spectra with simple Gaussians works only as long as a relevant part of the occurring transfer rates is not too much slower than τ_0. Otherwise, other transfer mechanisms such as transfer through vibrationally excited states may contribute significantly to the energy transfer.

Table 1 lists the results of the simulations. The first four columns give the spectral parameters used in each simulation. Note that only one of these four parameters is independent; Γ_{IDF} and Γ_{hom} are related through $\Gamma_{hom}^2 + \Gamma_{IDF}^2 = \Gamma_{tot}^2$, S is related to Γ_{hom} as in Eq. 4, and κ was defined as $\Gamma_{hom}/\Gamma_{IDF}$. The next column gives the shift after the excitation density has reached thermal equilibrium in a 5×5 system. Then two sets of columns give the time constants and amplitudes of the one- and two-exponential fit. The rms residues for the one-exponential fit were typically 1–2% of the maximal shift; for the two-exponential fit this was 0.1–0.3%. The final two columns give the average of the distribution of transfer times between neighboring subunits and the width of this distribution. These last two numbers were calculated for an antenna directly after nonselective excitation. Establishment of the equilibrium will lead to slower transfer rates becoming more prominent as will be shown below.

From the one-exponential fit we observe that the equilibration time converges to $\approx 0.5\ \tau_0$ for $\kappa \geq 1.5$. If we compare this with the average residence time $\tau_{av}/z = 1.3\ \tau_0/4 = 0.33\ \tau_0$, it appears that the time constant for the equilibration corresponds to ~1.5 hops in these cases of little inhomogeneous broadening.

For smaller κ the inhomogeneous energy distribution results in lower rates and slower phases in the equilibration process. Down to a ratio of 0.35 reasonable kinetics can be obtained. For even lower values of κ the kinetics slow down dramatically. For example, for $\kappa \leq 0.2$, with our model >55% of the transfer times are larger than 100 τ_0 and more than 50% of the equilibration is described by time constants larger than 100 τ_0 (data not shown). Under such circumstances other mechanisms can accelerate the transfer so that the results from our model will not be correct. Therefore we do not include these cases in our table.

As is observed in Table 1, the best fits to the magnitude of the shift are obtained for $\kappa \approx 0.6$. Therefore, we assume that this ratio will be between 0.5 and 0.7. In that case the equilibration rate as found from the one-exponential fit is 3.1–1.8 τ_0. If we compare this with the experimentally observed 325 fs we find that τ_0 = 100–150 fs. Both cases yield a distribution for the time of transfer between subunits with an average (τ_{av}) of 2.2–1.8 τ_0 = 220–270 fs and a width of 170 fs. Therefore a range of transfer rates between 100 and 500 fs should be expected. Fig. 7 gives the distribution of transfer rates for $\kappa = 0.7$.

One should realize that the average time that an excitation is at some subunit is τ_{av}/z, since every subunit is connected to z neighbors. This time τ_{av}/z is called the average residence time. Since an excitation makes a transfer step on the average every $\tau_{av}/z \approx 60$ fs, a time constant of 325 fs for the

TABLE 1 One- and two-exponential fit to the average redshift in a 5 × 5 LHA at 300 K (k_BT = 16 nm)

Parameters					Two-exponential fit					One-exponential fit			pigment-pigment transfer	
κ	Γ_{IDF} (nm)	Γ_{hom} (nm)	S (nm)	Shift (nm)	A_0 (nm)	τ_1/τ_0	A_1 (nm)	τ_2/τ_0	A_2 (nm)	A_0 (nm)	τ_1/τ_0	A_1 (nm)	τ_{av}/τ_0	σ_τ/τ_{av}
0.35	38	13	2	14.7	12.8	2.8	5.2	14	7.4	12.3	8.6	10.9	2.8	1.0
0.5	36	18	4	13.1	11.9	1.22	5.4	5.3	6.4	11.6	3.1	10.5	2.2	0.8
0.7	33	22	5.3	11.1	11.0	0.84	6.4	3.8	4.4	10.8	1.81	9.7	1.8	0.6
1	28	28	9	8.43	8.4	0.50	5.7	2.2	2.6	8.4	0.93	7.7	1.5	0.5
1.5	22	33	12	5.30	4.7	0.30	3.1	1.1	1.6	4.8	0.51	4.6	1.4	0.4
2.0	18	36	14	3.43	3.8	0.28	2.6	0.9	1.2	3.8	0.45	3.7	1.3	0.3

Parameters characterizing simulated energy transfer in the inhomogeneously broadened LH1 antenna. Γ_{hom} and Γ_{IDF} are the FWHM widths of the (Gaussian-modeled) homogeneous absorption spectrum and the IDF, respectively. All time constants are in units of τ_0, the optimal energy transfer time between two subunits. τ_{av} is the average energy-transfer time constant for two neighboring subunits. It should be realized that an excitation resides only τ_{av}/z on a single subunit on the average, with z the coordination number. For the employed square lattice in the simulation, $z = 4$. τ_{av}/z is called the average residence time. The best agreement with the observed shift was obtained for κ = 0.5–0.7.

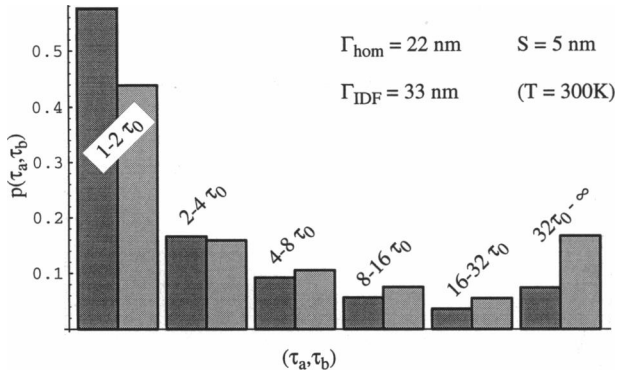

FIGURE 7 Distribution of transfer times in an inhomogeneously broadened LHA, directly after nonselective excitation (*left*) and after equilibration (*right*). Parameters are taken from the case $\kappa = 0.7$ in Table 1. Each bar represents a range (τ_a, τ_b) of times in units of τ_0. The height of the bar gives the probability $p(\tau_a, \tau_b)$ that a transfer time is in this range. It is obvious that after equilibration, slower transfer times become more prominent; however, more than 50% of the transfer times is still faster than 4 τ_0, corresponding to 400–600 fs.

equilibration corresponds to ~5 hops on the average. After 5 hops, a randomly hopping excitation will be removed from its starting position by $\sqrt{5}$ lattice distances. This is of the order of the size of the lattices we employed in the simulations (5 × 5). Below we will demonstrate that for larger lattices, similar results are obtained. Here we can conclude that upon larger inhomogeneous broadening, the equilibration requires a longer time and involves more subunits, in agreement with physical intuition. An average residence time of 60 fs corresponds to a (homogeneous) lifetime broadening of 8.6 nm ($\Gamma_{lifetime}$, FWHM) at these wavelengths. This is smaller than the total homogeneous bandwidth Γ_{hom} of ~21 nm (Table 1) in the simulations for $\kappa = 0.6$, as it should be.

Since our estimate of τ_0 = 100–150 fs is faster than previous results, it is useful to analyze it in terms of the Förster transfer mechanism. The standard approach needs an additional term to correct for the different homogeneous bandwidths that we have used in our estimates. This can be done by assuming a constant dipole strength. The optimal transfer time between two subunits at a distance r is given by: $\tau_0 = \tau_{op}(\Gamma_{hom}/\Gamma_0)(r/R_0)^6$, where τ_{op} = 15 ns (see, e.g., Bakker et al., 1983) is the radiative lifetime of the subunit, R_0 is the Förster radius, and Γ_0 the width of the band for which R_0 was determined. From monomeric BChl-*a* (ε_{773} = 90/(mM cm), Γ_0 = 35 nm (Hoff and Amesz, 1991) and using $n = 1$ for the refractive index and the value 5/4 for the orientation factor (random organization in a plane), we obtain R_0 = 13 nm (Förster, 1965). For κ = 0.5–0.7 we find r = 2.0–2.1 nm. An additional correction is necessary because the subunit in our case is a dimer. This correction may be obtained by using a twice larger value for the spectral overlap and a twice smaller value for τ_{op}. In this case the estimate for the subunit distance has to be increased by a factor $4^{1/6}$ = 1.26 to r = 2.5–2.7 nm. For these parameters, the excitonic dipole-dipole interaction equals 21–26 cm^{-1} (which corresponds to 1.6–2.0 nm around wavelengths of 880 nm). It is not *a priori* clear which value for the refractive index should be used. Using $n = 2$ results in 40% smaller distances. The exciton splitting, however, is not affected. The calculated excitonic dipole-dipole interaction is considerably less than the inhomogeneous broadening (33–35 nm), which demonstrates that even though some very fast transfer occurs in our model, the major part of the subunits remains in the weak coupling limit, and the approach that we have used in this paper, to calculate the transfer times from spectral overlap, remains justified. Furthermore, the dimer-dimer exciton interaction is very small compared with the values of Γ_{IDF}, which justifies our treatment of the energy transfer process in terms of Förster transfer between dimers. The dimer-dimer distances obtained from the calculation (using $n = 1$) agree with a model in which 12 subunits are distributed equally over a ringlike structure with a radius of 4 nm. Such structures have been observed by electron microscopy for light-harvesting antenna-RC core complexes of *Rps. viridis* (Miller, 1982) and more recently for *Rps. marina* (Meckenstock et al., 1992) and *Rs. molischianum* (Boonstra et al., 1994). The structures of RC-less LH1 complexes of *Rb. sphaeroides* as reported in Boonstra et al. (1993) are somewhat smaller with a diameter of 52 Å; however, these complexes may not be the aggregation form that occurs in vivo.

Between subunits of neighboring core complexes such distances are only possible if these complexes are rather tightly packed, which was observed for *Rps. viridis* (Miller, 1982). Otherwise the transfer within core complexes will be much faster than between them, giving rise to a one-dimensional equilibration process. However, strong conclusions about the connectivity between different core complexes cannot be made from our observations, as the observed shifting of the difference spectra can already be explained by an equilibration over only 25 subunits.

Although a reasonable estimate of the equilibration could be obtained by a one-exponential fit, Table 1 also demonstrates that the kinetics of the equilibration is inherently multiexponential. The two-exponential fit describes the kinetics considerably better than the one-exponential fit, as can be seen from the rms of the residues. This is demonstrated in Fig. 8, which shows the simulated equilibration kinetics for $\kappa = 0.7$, with a one- and two-exponential fit. In addition we note from the amplitudes of the two-exponential fit to the simulated shift kinetics (in Table 1) that at $\kappa \leq 0.5 > 10\%$ of the shift occurs at a time scale slower than the time window of our simulation (of 20 τ_0). One reason for this multiexponentiality is the distribution of transfer times between the individual subunits. A second reason is the spectral inhomogeneity itself, because of which some excitations need more steps to reach equilibrium than others. However, although our data (Fig. 2) show some signs of the presence of more than one decay time, the experimental uncertainties are too large to make a reasonable estimate of the amplitudes and decay times. Moreover, it is doubtful

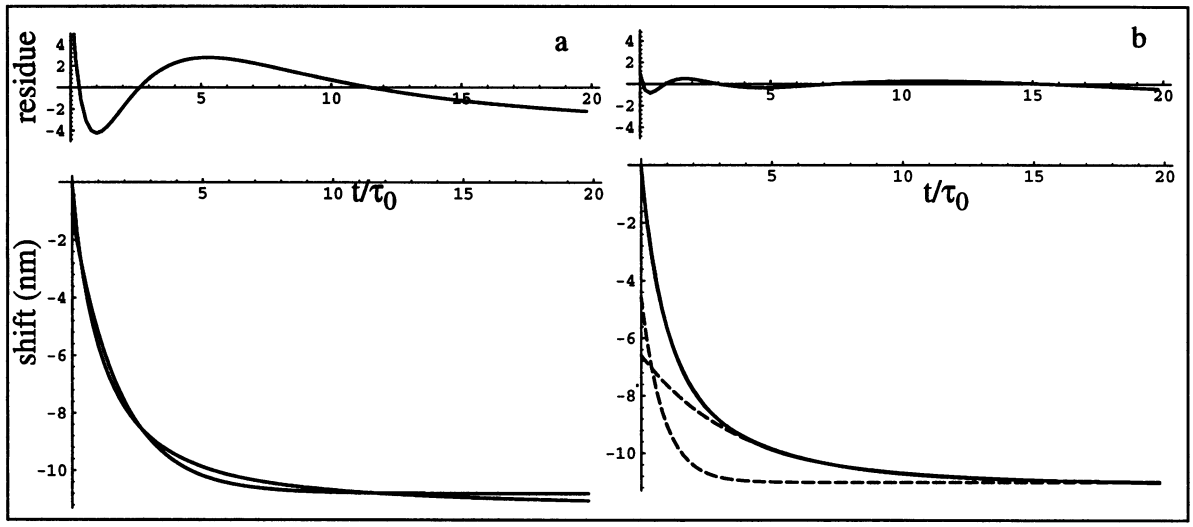

FIGURE 8 One- (*a*) and two-exponential (*b*) fit to the simulated shift of the energy distribution over the subunits after homogeneous excitation. Here, $\kappa = 0.7$. *Lower plots*; (——) data and fit. (- - - -) components of the fit. *Upper plots*: residue in percents of the maximal shift. A one-exponential fit yields a residue of maximally 4% of the final shift. For the two-exponential fit this is 1%.

whether our simplified spectral model gives a good calculation of these variables.

Simulations on different lattices

It has been argued (Van Mourik, 1993, Pullerits, 1994b) that in addition to the initial equilibration where the excitation migrates to a nearby area of subunits at a relatively low energy, a slower equilibration takes place between such areas, especially at low temperatures. This process is partly neglected when applying periodic boundary conditions as was done in our simulations. To estimate the influence of this effect on the kinetics of the equilibration, we carried out simulations with square antenna lattices varying from 3×3 to 10×10 subunits (results not shown). Indeed, for $\kappa = 0.7$, a decrease of the antenna size from 5×5 to 3×3 led to a 20% increase of the equilibration rate. However, an increase from 5×5 to 10×10 subunits gave a <5% decrease. Therefore it turns out that in this case, little equilibration takes place on a longer range than 5×5 sites and thus our analysis remains valid, at least for LH1 at room temperature.

A second factor that influences the equilibration rate is the structure of the light-harvesting antenna (LHA). To investigate this we carried out simulations in hexagonal lattices of various sizes (data not shown). In all cases the equilibration was ~1.5 times faster than on the square lattice. This agrees with the coordination number, which is also 1.5 times larger ($z = 6$ instead of 4). In a lattice with 12 subunits per RC, the average coordination number is 4.5 (see, e.g., Somsen et al., 1994) and indeed, the equilibration was only slightly faster than on a square lattice. It therefore seems most proper to scale the equilibration rate with the coordination number. This will only give problems in extreme cases (e.g., $z = 1$ or very large z). So, an analysis of our data with a hexagonal lattice will lead to a 50% higher estimate for τ_0, and leave the average residence time on a single subunit almost unchanged.

Dimer pairs in LH1?

So far we have treated the LHA as a structurally homogeneous lattice of 12 pigment dimers per LHA-RC unit. However, a structurally inhomogeneous organization for the LHA has been proposed (Scherz and Parson, 1986) suggesting that the dimers are organized in six pairs. The dimers within a pair could be relatively close allowing for faster transfer between them than between dimers of different pairs. Such an arrangement then could give rise to two time scales of equilibration, first within and then between dimer pairs.

The equilibration process we observed can be either of the two processes or both. However, the size of the equilibration shift depends on the inhomogeneous bandwidth, the temperature, and the number of connected subunits. Since the inhomogeneous bandwidth is less than the total bandwidth ($\Gamma_{IDF} < \Gamma_{tot} = 40$ nm), an equilibrium shift of 12 nm at room temperature can only be explained if five or more subunits are connected, as can be seen from the lower curve in Fig. 6. Therefore, the observed equilibration cannot be an equilibration within dimer pairs only. Moreover, if this would be the case, a slower equilibration phase between the dimer pairs should be observed, which is not the case.

The second option is that the equilibration we observed is only the equilibration between pairs and that it was preceded by a faster equilibration within dimer pairs that we did not observe. In that case the equilibrium shift is larger than the shift we observed, since we then observed only the difference in equilibrium shift between dimer pairs and the total system. With the same method as applied above, this

then leads us to estimate $\Gamma_{IDF} = 42$ nm, resulting in a total shift of 18 nm for the total system and a shift of 6 nm between the dimer pairs. Since now $\Gamma_{IDF} > \Gamma_{tot}$, we have a problem with our analysis. This case would imply that the homogeneous bands are extremely narrow and would lead consequently to a slower simulated equilibration and therefore to an even smaller estimate for τ_0. As a consequence, the distances between the pairs of dimers would become unreasonably short, and we would thereby lose the concept of closely associated dimer pairs. A possible way out is that the second process, transfer between pairs of dimers, is associated with a large coordination number ($z \geq 4$), while the transfer within pairs corresponds to a $z = 1$ process. In that case, both processes are mixed in the equilibration. However, the observed 300 fs fluorescence depolarization (S. Bradforth, R. Jimenez, F. Van Mourik, R. Van Grondelle, and G. R. Fleming, submitted for publication) may still predominantly arise within dimer pairs.

At this stage we want to emphasize that the decay of the fluorescence anisotropy is a different process from the equilibration of the excitation energy and could be both faster or slower depending on the actual structure of the antenna, and further analysis should wait for a more definitive structural model.

Artifacts in the simulations and limitations of the experimental data

We have tried to explain the observed equilibration using a simplified model with a minimal set of parameters. However, our simplifications give rise to at least two possible artifacts. First of all, the condition of detailed balance combined with our choice of Gaussian band shapes results in a relation between homogeneous bandwidth, temperature and Stokes' shift Eq. 4. We have used the approach to vary the homogeneous bandwidth and set the Stokes' shift to satisfy this relation. However, the quadratic dependence has forced us to vary the Stokes' shift over a rather broad range (see Table 1). The resulting changes in the kinetics are only partly due to the change in homogeneous bandwidth. They are also effected by the Stokes' shift, which makes it more difficult to understand what is really happening. A larger Γ_{hom} means a smaller Γ_{IDF}, and thus a smaller total shift. A larger Γ_{hom} also leads to a larger value of the Stokes' shift S, and thus to a faster equilibration. This second effect could be called an artifact. It arises from constraint (Eq. 4). The fluorescence maximum of *Rs. rubrum* LH1 at room temperature occurs at 900 nm. This is 17 nm toward the infrared of the absorption maximum (883 nm) (Rijgersberg, 1980). Of this difference, 12 nm can be explained by the transient redshift of the spectrum due to equilibration of the excitation density. The remaining 5 nm could be due to the Stokes' shift of the individual subunits. In the case of the isolated B820 complexes, which show no energy transfer, the fluorescence maximum is at 825 nm, which is 5 nm to the infrared of the absorption maximum at 820 nm.

Thus, the value of 4–5.3 nm obtained for S from our simulations (see Table 1) seems realistic and consistent with the view that the difference between fluorescence and absorption maximum is made up of a shift due to equilibration via energy transfer on the low energy subunits (12 nm) and a Stokes' shift of every individual subunit (5 nm).

A second cause for artifacts is the choice of Gaussian band shapes for both absorption and emission spectra, which do not include both the presence of 0–0 transitions and vibrational sub-bands. The former poses a problem if the Stokes' shift is larger than both the homogeneous and the inhomogeneous bandwidth. In such a case the transfer rate between any pair of subunits is almost equally slow in the simulations. In reality, a significant amount of transfer could take place through the 0–0 transitions of subunits at identical energy in the IDF. The absence of vibrational sub-bands causes an artifact in the case when the homogeneous band is much narrower than the inhomogeneous distribution. In that case transfer from blue-shifted subunits to neighbors that are more than a Stokes' shift lower in energy may take place for a relevant part through the vibrational side-bands of the acceptor. An example of such a case may be the B800 → B850 transfer in LH2 (Van der Laan et al., 1990; Reddy et al., 1991). Both these artifacts underestimate the transfer rates. For LH1 at room temperature, our estimates seem to be reasonably valid; the Stokes' shift is substantially smaller than both Γ_{hom} and Γ_{IDF}, which are on the same order of magnitude. Moreover, at room temperature the 0–0 line is neglible with respect to the phonon wing. However, estimates at cryogenic temperatures ($<<$ 100 K) should be done with great care. Inclusion of additional bands would improve the validity of the model; however, we believe it would not improve our understanding of the equilibration process.

As mentioned, sub-100 fs phases in the shifting of the ΔOD spectra are washed out for a significant part because of the instrument response. However, in our model, a maximal shift of 17.5 nm is possible after "homogeneous excitation." This is for the (unphysical) case of $\kappa = 0$. For larger κ, as is seen from combining (Eq. 1) with the constraint $\Gamma^2_{hom} + \Gamma^2_{IDF} = \Gamma^2_{tot}$, the shift is smaller by a factor $1/(1 + \kappa^2_y)$. For physically reasonable values of κ, e.g., $\kappa > 0.3$, the shift is $<$16 nm. We therefore expect that experiments with higher time resolution will not yield much larger shifts than the 12 nm we observed, unless selective excitation is done, e.g., in the high energy side of the Q_y absorption band. If one would claim that some shift in the B820 data (Fig. 3) is hidden in the noise, then the much larger observed shift in the LH1 antenna is partly due to such interdimer shift. One could still apply the analysis described above, but the shift due to energy transfer would be the observed shift in LH1 minus the value found in B820. Since we estimate the maximal shift possibly hidden by remaining noise in the dataset from which Fig. 3 was taken to be 3 nm, the shift due to energy transfer is then at least 9 nm.

Comparison with other experiments and other light-harvesting systems

Our current estimate of the average hopping time τ_{av} = 200–300 fs is in reasonable agreement with earlier estimates based on bi-excitation annihilation kinetics (Bakker et al., 1983, Valkunas et al., 1986). As mentioned before, the inhomogeneity in the antenna absorption was not accounted for in these papers. In a subsequent paper we will accurately measure and analyze the time-resolved annihilation kinetics. A preliminary analysis shows that these are also consistent with the estimated value for τ_0 and τ_{av}. The obtained values for Γ_{IDF} and Γ_{hom} in LH1 are very similar to the values (extrapolated from 77 K to room temperature) from the analysis of the energy-selective fluorescence measurements on the B820 subunit (Pullerits et al., 1994a), but contrast strongly with the values suggested for LH1 at room temperature (Pullerits et al., 1994b). However, the experimental transient absorption data in the latter paper were obtained with a ~12 ps FWHM instrument response, so that any sub-ps equilibration phenomenon is washed out.

Recently the time-resolved depolarization of the fluorescence on LH1-only membranes was measured. A 300 fs depolarization process was observed, remarkably similar to the time constant of the zero-crossing kinetics (S. Bradforth, R. Jimenez, F. Van Mourik, R. Van Grondelle, and G. R. Fleming, submitted for publication). Within the framework of the model analysis above this implies that the time constant for the polarization decay to the long-time value (r(infinite) = 0.07) corresponds to four to five transfer steps on the LH1 lattice on the average.

Very recently, a similar fast shifting of the transient bleaching spectra in membranes of a LH1-only *Rb. capsulatus* mutant was reported (Xiao et al., 1994). The 0-transition shifts from ~846 to 866 nm with a time constant of 250–400 fs after excitation in the high energy side of the LH1 absorption at 800 nm. We note that in the model for *Rs. rubrum* LH1 presented here, one expects a larger shift upon high-energy-edge excitation than upon Q_x excitation as was done in our experiment reported here. Xiao et al. (1994) tentatively explained their observation by a relaxation between delocalized electronic states. In view of the amount of disorder relative to the excitonic coupling between dimer pairs it seems unlikely that any delocalization beyond the level of dimers takes place in these systems (Fidder et al., 1991). In addition, so far low-temperature polarized light spectroscopy and energy-selective spectroscopy have failed to detect excitonic states within the LH1 absorption profile (e.g., Van Mourik et al., 1992b), and in fact most of the experimental evidence available supports the dimer-to-dimer energy transfer model as used here.

The time-constant for spectral equilibration observed by us is very similar to that obtained for spectral equilibration within the Fenna-Matthews-Olson (FMO) trimer of *Chlorobium tepidum* (Savhikin et al., 1994). It is about a factor of 6 faster than the value observed in the antenna of *Heliobacillus mobilis* (Lin et al., 1994), which might be due to the fact that in this species the spectral equilibration process is in fact rather multiphasic, with both a sub-picosecond and a picosecond phase, possibly due to the strong heterogeneous spectral composition of this antenna. Similar bi- or multiphasic spectral equilibration processes have been observed in PS1 with a sub-ps process in the major antenna followed by excitation equilibration between the bulk antenna components and some fraction of lower energy pigments (Lin et al., 1992; Holzwarth et al., 1993). Also in an LH-1-only mutant of *Rb. sphaeroides*, which contains LH1 as the only pigment-protein complex, we observed multiphasic equilibration kinetics with a strong ~600 fs process followed by a minor (<15%) phase of a few picoseconds (H.M. Visser, O. J. G. Somsen, F. Van Mourik, and R. Van Grondelle, in preparation).

Trapping by the RC

The preferential localization of the excited state on low energy states within LH1 may be of importance for the functioning of photosynthetic organisms in vivo. It seems to exclude a model in which the excitation energy is delocalized over all antenna subunits to the same extent during the trapping by the RC in *Rs. rubrum*. To investigate the consequences of this idea, we calculated the distribution of transfer times after equilibration. The probability that a subunit at a specific energy is excited is now proportional to the shifted IDF (product of Boltzman distribution and IDF). The result is shown in Fig. 7, for the case of κ = 0.7. Upon comparison with the initial distribution, it is clear that slower transfer times are more prominent after equilibration, but at room temperature the effect is weak, and >50% of the transfer times is still less than 4 τ_0, amounting to 400–600 fs in our description. Therefore, local trapping effects are not strong at room temperature, and slow transfer to the RC must arise from a different source. We believe that the major reason for this slow transfer to P in comparison with the fast transfer within LH1 is the distance between the LH1 pigments (or LH1 dimers) and P (see Somsen et al., 1994). However, in other photosynthetic systems, e.g., PS1 of green plants (Trinkunas and Holzwarth, 1994), or in *Heliobacillus mobilis* this situation may be totally different. Also in *Rs. rubrum* and other light-harvesting systems at low temperatures the local trapping of the excitations on low energy pigments may limit the efficiency of the trapping process.

SUMMARY

To summarize, the view that we obtain on the energy transfer dynamics in the antenna system of *Rs. rubrum* is drastically different from that of many previous studies, in which the effect of the inhomogeneous energy distribution was supposed to be negligible at room temperature. To describe the experimental data, we find the ratio κ of the homogenous bandwidth over the inhomogeneous bandwidth

to be to 0.6 ± 0.1. An average pairwise energy transfer time of 200–300 fs is obtained, in reasonable agreement with estimations from fast depolarization measurements (S. Bradforth, R. Jimenez, F. Van Mourik, R. Van Grondelle, and G. R. Fleming, submitted for publication) and annihilation measurements (Bakker et al., 1983; Deinum et al., 1989). Therefore, an average residence time of an excitation on a subunit of 50–70 fs is found, and the 325 fs time constant for the equilibration corresponds to ~5 hops. Since the observed equilibration could not be resolved in previous experiments, models for LH1 describing those experimental data resulted in very different parameters (Pullerits et al., 1992, 1994b). It seems likely that equilibration phenomena similar to the one described here can be observed in many photosynthetic antenna systems that have similar inhomogeneously broadened absorption bands.

This research was supported by EEC grants CT 92 0796 and CT 93 0278, and by the Dutch Organization for Scientific Research through the Dutch Foundation for Life Sciences. S. L. gratefully acknowledges a visitor fellowship from the Free University.

REFERENCES

Aagard, J., and W. R. Sistrom. 1972. Control of synthesis of reaction center bacteriochlorophyll in photosynthetic bacteria. *Photochem. Photobiol.* 15:209–225.

Allen, J. P., G. Feher, T. O. Yeates, H. Komiya, and D. C. Rees. 1987. Structure of the reaction center from *Rhodobacter sphaeroides* R-26: the cofactors. *Proc. Natl. Acad. Sci. USA.* 84:5730–5734.

Bakker, J. C. G., R. van Grondelle, and W. T. F. den Hollander, 1983. Trapping, loss and annihilation of excitations in a photosynthetic system II. Experiments with the purple bacteria *Rhodospirillum rubrum* and *Rhodopseudomenas capsulatus*. *Biochim. Biophys. Acta* 725:508–518.

Becker, M., V. Nagarajan, and W. W. Parson. 1991. Properties of the excited-singlet states of bacteriochlorophyll *a* and Bacteriopheophytin *a* in polar solvents. *J. Am. Chem. Soc.* 113:6840–6848.

Beekman, L. B., F. van Mourik, M. R. Jones, H. M. Visser, and R. van Grondelle. 1994. Trapping kinetics of the photosynthetic purple bacterium *Rhodobacter sphaeroides:* influence of the charge separation rate and consequences for the rate-limiting step in the light harvesting process. *Biochemistry.* 33:3143–3147.

Boonstra, A. F., L. Germeroth, and E. J. Boekema. 1994. Structure of the light harvesting antenna from *Rhodospirillum molischianum* studied by electron microscopy. *Biochim. Biophys. Acta.* 1184:227–234.

Boonstra, A. F., R. W. Visschers, F. Calkoen, R. van Grondelle, E. F. J. van Bruggen, and E. J. Boekema. 1993. Structural characterization of the B800–850 and B875 light-harvesting antenna complexes from *Rhodobacter sphaeroides* by electron microscopy. *Biochim. Biophys. Acta.* 1141:181–188.

Chang, M. C., P. M. Callahan, P. S. Parkes-Loach, T. M. Cotton, and P. A. Loach. 1990. Spectroscopic characterization of the light-harvesting complex of *Rhodospirillum rubrum* and its structural subunit. *Biochemistry.* 29:421–429.

Deinum, G., T. J. Aartsma, R. van Grondelle, and J. Amesz. 1989. Singlet-singlet annihilation measurements in the antenna of *Rhodospirillum rubrum* between 300 and 4 K. *Biochim. Biophys. Acta.* 976: 63–69.

Deisenhofer, J., O. Epp, K. Miki, R. Huber, and H. Michel. 1984. X-ray structure analysis of a membrane protein complex. Electron density map at 3 Å resolution and a model of the chromophores of the photosynthetic reaction center from *Rhodopseudomonas viridis*. *J. Mol. Biol.* 180: 385–398.

Den Hollander, W. Th. F., J. G. C. Bakker, and R. van Grondelle. 1983. Trapping, loss and annihilation of excitations in a photosynthetic system. I. Theoretical aspects. *Biochim. Biophys. Acta.* 725:508–518.

Du, M., S. J. Rosenthal, X. Xie, T. J. DiMagno, M. Schmidt, D. K. Hanson, M. Schiffer, J. R. Norris, and G. R. Fleming. 1992. Femtosecond spontaneous-emission studies of reaction centers from photosynthetic bacteria. *Proc. Natl. Acad. Sci. USA.* 89:8517–8521.

Du, M., X. Xie, L. Mets, and G. Fleming. 1994. Direct observation of elementary energy transfer processes in light harvesting complex. *J. Phys. Chem.* 98:4736–4741.

Du, M., X. Xie, Y. Jia, L. Mets, and G. R. Fleming. 1993. Direct observation of ultrafast energy transfer in PSI core antenna. *Chem. Phys. Lett.* 201:535–542.

Eads, D. D., E. W. Castner Jr., R. S. Alberte, L. Mets, and G. R. Fleming, 1989. Direct observation of energy transfer in a photosynthetic membrane: chlorophyll b to chlorophyll a transfer in LHC. *J. Phys. Chem.* 93:8271–8275.

Fidder, H., J. Knoester, and D. A. Wiersma. 1991. Optical properties of disordered molecular aggregates: a numerical study. *J. Chem. Phys.* 95:7880–7890.

Fleming, G. R. 1986. Chemical Applications of Ultrafast Spectroscopy. Oxford University Press, New York. 82–85.

Förster, T. 1965. Delocalized excitation and excitation transfer. *In* Modern Quantum Chemistry, Vol. 3. O. Sinanoglu, editor. Academic Press, New York. 93–137.

Freiberg, A., V. I. Godik, and K. Timpmann. 1987. Spectral dependence of the fluorescence lifetime of *Rhodospirillum rubrum*. Evidence for inhomogeneity of B880 absorption band. *In:* Progress in Photosynthesis Research, Vol. 1. J. Biggins, editor. Marinus Nijhoff Publisher, Dordrecht, The Netherlands. 45–48.

Gobets, B., H. van Amerongen, R. Monshouwer, J. Kruip, M. Rögner, R. van Grondelle, and J. P. Dekker. 1994. Polarized site-selected fluorescence spectroscopy of isolated photosystem I particles. *Biochim. Biophys Acta.* 1188:75–85.

Greene, B. J., and R. C. Farrow. 1983. The subpicosecond Kerr effect in CS_2. *Chem. Phys. Lett.* 98:273–275.

Hess, S., K. J. Visscher, V. Sundström, G. J. S. Fowler, and C. N. Hunter. 1994. Enhanced rates of sub-ps energy transfer in blue-shifted light-harvesting LH2 mutants of *Rb. sphaeroides*. *Biochemistry.* 33: 8300–8305.

Hoff, A. J., and J. Amesz. 1991. Visible absorption spectroscopy of chlorophylls. In Chlorophylls. H. Scheer, editor. CRC Handbook, CRC Press, Boca Raton, FL. 723–738.

Holzwarth, A. R. 1991. Excited state kinetics in chlorophyll systems and its relationship to the functional organization of the photosystems. *In* Chlorophylls. H. Scheer, editor. CRC Handbook, CRC Press, Boca Raton, FL. 1125–1152.

Holzwarth, A. R., G. Schatz, H. Brock, and E. Bittersmann. 1993. Energy transfer and charge separation kinetics in photosystem I. 1. Picosecond transient absorption and fluorescence study of cyanobacterial photosystem I particles. *Biophys. J.* 64:1813–1826.

Hunter, C. N., R. van Grondelle, and J. D. Olsen. 1989. Photosynthetic antenna proteins: 100 ps before photochemistry starts. *Trends Biochem. Sci.* 14:72–76.

Jean, J. M., C.-K. Chan, G. R. Fleming, and T. G. Owens. 1989. Excitation transport and trapping on spectrally disordered lattices. *Biophys. J.* 56:1203–1215.

Knapp, E. W. 1984. Lineshapes of molecular aggregates. Exchange narrowing and intersite correlation. *Chem. Phys.* 85:73–85.

Koolhaas, M. H. C., F. van Mourik, G. van der Zwan, and R. van Grondelle. 1994. The B820 subunit of the bacterial light-harvesting antenna: a dis-ordered dimer? *J. Lumin.* 60, 61:515–519.

Kramer, H. J. M., J. Pennoyer, R. van Grondelle, W. H. J. Westerhuis, R. A. Niederman, and J. Amesz. 1984. Low temperature optical properties and pigment organization of the B875 light-harvesting bacteriochlorophyll complex of purple photosynthetic bacteria. *Biochim. Biophys. Acta.* 767:156–165.

Kühlbrandt, W., D. N. Wang, and Y. Fujiyoshi. 1994. Atomic model of plant light-harvesting complex. *Nature.* 367:614–621.

Lin, S., H.-C. Chiou, F. A. M. Kleinherenbrink, and R. E. Blankenship. 1994. Time-resolved spectroscopy on energy and electron transfer pro-

cesses in the photosynthetic bacterium *Heliobacillus mobilis*. *Biophys. J.* 66:437–445.

Lin, S., H. van Amerongen, and W. S. Struve. 1992. Ultrafast pump-probe spectroscopy of the P700 and F_x-containing Photosystem I core protein from *Synechococcus* sp. PCC 6301 (*Anacystis nidulans*). *Biochim. Biophys. Acta.* 1140:6–14.

Matthews, B. W., R. E. Fenna, M. C. Bolognesi, M. F. Schmid, and J. M. Olson. 1979. Structure of the Bacteriochlorophyll-*a* Protein from *Rhodopseudomenas marina*. 1. Purification and characterization. *FEBS Lett.* 311:135–138.

McDermott, G., S. M. Prince, A. A. Freer, A. M. Hawthornthwaite-Lawless, M. Z. Papiz, R. J. Cogdell, and N. W. Isaacs. 1995. Crystal structure of an integral membrane light-harvesting complex from photosynthetic bacteria. *Nature.* 374:517–521.

Meckenstock, R. U., K. Kruche, R. A. Brunisholz, H. Zuber. 1992. The light-harvesting core-complex and the B820-subunit from *Rhodopseudomonas marina*. 2. Electron microscopic characterization. *FEBS Lett.* 311:135–138.

Miller, J. F., P. S. Parkes-Loach, P. M. Callahan, J. R. Sprinkle, and P. A. Loach. 1987. Isolation and characterization of a subunit form of the light-harvesting complex of *Rhodospirillum rubrum*. *Biochemistry.* 26: 5055–5062.

Miller, K. R. 1982. Three-dimensional structure of a photosynthetic membrane. *Nature.* 300:53–55.

Nuijs, A. N., R. van Grondelle, H. L. P. Joppe, A. C. van Bochove, and L. N. M. Duysens. 1985. Singlet and triplet excited carotenoid and antenna bacteriochlorophyll of the photosynthetic purple bacterium *Rhodospirillum rubrum* as studied by picosecond absorbance difference spectroscopy. *Biochim. Biophys. Acta.* 810:94–105.

Owens, T. G., S. P. Webb, L. Mets, R. S. Alberte, and G. R. Fleming. 1987. Antenna size dependence of the fluorescence decay in the core antenna of photosystem I: estimates of charge separation and energy transfer rates. *Proc. Natl. Acad. Sci. USA.* 84:1532–1536.

Paillotin, G., C. E. Swenberg, J. Breton, and N. E. Geacintov. 1979. Analysis of picosecond laser-induced fluorescence phenomena in photosynthetic membranes utilizing a master equation approach. *Biophys. J.* 25:513–534.

Pearlstein, R. M. 1991. Theoretical interpretation of antenna spectra. *In* Chlorophylls. H. Scheer, editor. CRC Handbook, CRC Press, Boca Raton, FL. 1047–1078.

Pullerits, T., and A. Freiberg. 1992. Kinetic model of primary energy transfer and trapping in photosynthetic membranes. *Biophys. J.* 63: 879–896.

Pullerits, T., F. van Mourik, R. Monshouwer, R. W. Visschers, and R. van Grondelle. 1994a. Electron Phonon coupling in the B820 subunit form of LH1 studied by temperature dependence of optical spectra. *J. Lumin.* 58:168–171.

Pullerits, T., K. J. Visscher, S. Hess, V. Sundström, A. Freiberg, K. Timpmann, and R. van Grondelle. 1994b. Energy transfer in the homogeneously broadened core antenna of purple bacteria: a simultaneous fit of low-intensity picosecond absorption and fluorescence kinetics. *Biophys. J.* 66:236–248.

Reddy, N. R. S., P. A. Lyle, and G. J. Small. 1992. Applications of spectral hole-burning spectroscopy to antenna and reaction center complexes. *Photosynth. Res.* 31:167–194.

Reddy, N. R. S., G. J. Small, M. Seibert, and R. Picorel. 1991. Energy transfer dynamics of the B800–B850 antenna complex of *Rhodobacter sphaeroides:* a hole burning study. *Chem. Phys. Lett.* 181:391–399.

Rijgersberg, C. P., R. van Grondelle, and J. Amesz. 1980. Energy transfer and bacteriochlorophyll fluorescence in purple bacteria at low temperature. *Biochim. Biophys. Acta.* 592:53–64.

Savikhin, S., W. Zhou, R. E. Blankenship, and W. S. Struve. 1994. Femtosecond energy transfer in Bacteriochlorophyll-*a* protein trimers from the green bacterium *Chlorobium tepidum*. *Biophys. J.* 66:110–114.

Scherz, A., and W. W. Parson. 1986. Interactions of the bacteriochlorophyll-protein complexes of photosynthetic bacteria. *Photosynth. Res.* 9, 21.

Sevilla, J. M., M. Dominguez, F. Garica-Blanco, and M. Blazquez. 1989. Resolution of absorption spectra. *Comput. Chem.* 13:197–200.

Shreve, A. P., J. K. Trautman, T. G. Owens, and A. C. Albrecht. 1991. Determination of the S_2 lifetime of β-carotene. *Chem. Phys. Lett.* 178: 89–96.

Somsen, O. J. G., F. van Mourik, R. van Grondelle, and L. Valkunas. 1994. Energy migration in a spectrally and spatially inhomogeneous light-harvesting antenna. *Biophys. J.* 66:1580–1596.

Sundström, V., R. van Grondelle, H. Bergström, E. Åkeson, and T. Gilbro. 1986. Excitation-energy transport in the bacteriochlorophyll antenna systems of *Rhodospirillum rubrum* and *Rhodobacter sphaeroides*, studied by low-intensity picosecond absorption spectroscopy. *Biochim. Biophys. Acta.* 851:431–446.

Sundström, V., and R. van Grondelle. 1991. Dynamics of excitation energy transfer in photosynthetic bacteria. *In* Chlorophylls. H. Scheer, editor. CRC Handbook, CRC Press, Boca Raton, FL. 1125–1152.

Taguchi, A. K. W., J. W. Stocker, R. G. Alden, T. P. Causgrove, J. M. Peloquin, S. G. Boxer, and N. M. Woodbury. 1992. Biochemical characterization and electron transfer reactions of *symI*, a *Rhodobacter capsulatus* reaction center symmetry mutant which affects the initial electron donor. *Biochemistry.* 31:10345–10355.

Timpmann, K., and A. Freiberg. 1991. Picosecond kinetics of light excitations in photosynthetic purple bacteria in the temperature range of 300–4 K. *Chem. Phys. Lett.* 182:617–622.

Timpmann, K., F. G. Zhang, A. Freiberg, and V. Sundström. 1993. Detrapping of excitation energy from the reaction centre in the photosynthetic purple bacterium *Rhodospirillum rubrum*. *Biochim. Biophys. Acta.* 1183:185–193.

Trautman, J. K., A. P. Shreve, C. A. Violette, H. A. Frank, T. G. Owens, and C. A. Albrecht. 1990. Femtosecond dynamics of energy transfer in B800–850 light-harvesting complexes of *Rhodobacter sphaeroides*. *Proc. Natl. Acad. Sci. USA.* 87:215–219.

Trinkunas, G., and A. R. Holzwarth. 1994. Kinetic modeling of exciton migration in photosynthetic systems. 2. Simulations of excitation dynamics in two-dimensional photosystem 1 core antenna/reaction center complexes. *Biophys J.* 66:415–429.

Valkunas, L., S. Kudzmauskas, and V. Liuolia. 1986. Noncoherent migration of excitons in impure molecular structures. *Sov. Phys. Coll.* 26: 1–11.

Van der Laan, H., T. Schmidth, R. W. Visschers, K. J. Visscher, R. van Grondelle, and S. Völker. 1990. Energy transfer in the B800–850 antenna complex of purple bacteria *Rhodobacter sphaeroides:* a study by spectral hole-burning. *Chem. Phys. Lett.* 170:231–238.

Van Grondelle, R., H. Bergström, V. Sundström, R. J. van Dorssen, M. Vos, and N. Hunter. 1987. Energy transfer within the bacteriochlorophyll antenna of purple bacteria at 77 K studied by picosecond absorption recovery. *Biochim. Biophys. Acta.* 894:313–326.

Van Grondelle, R., J. P. Dekker, T. Gillbro, and V. Sundström. 1994. Energy transfer in photosynthesis. *Biochim. Biophys. Acta.* 1187:1–65.

Van Mourik, F. 1993. Spectral inhomogeneity of the bacterial light harvesting antenna: causes and consequences. Ph. D. thesis. Vrije Universiteit, Amsterdam, the Netherlands. 128 pp.

Van Mourik, F., E. Corten, I. H. M. van Stokkum, R. W. Visschers, R. Kraayenhof, and R. van Grondelle. 1992a. Self-assembly of the LH-1 light-harvesting antenna of *Rhodospirillum rubrum:* a time resolved study of the aggregation of the B820 subunit. *In* Research in Photosynthesis N. Murarata ed., Kluwer Academic Publishers, Dordrecht, The Netherlands. 101–104.

Van Mourik, F., J. R. van der Oord, K. J. Visscher, P. S. Parkes-Loach, P. A. Loach, R. W. Visschers, and R. van Grondelle. 1991. Exciton interactions in the light-harvesting antenna of photosynthetic bacteria studied with triplet-singlet spectroscopy and singlet-triplet annhilation in the B820 subunit form of *Rhodospirillum rubrum*. *Biochim. Biophys. Acta.* 1059:111–119.

Van Mourik, F., R. W. Visschers, and R. van Grondelle. 1992b. Energy transfer and aggregate size effects in the inhomogeneously broadened antenna core light harvesting antenna of *Rhodobacter sphaeroides*. *Chem. Phys. Lett.* 193:1–7.

Van Mourik, F., K. J. Visscher, J. Mulder, and R. van Grondelle. 1993. Spectral inhomogeneity of the light-harvesting antenna of *Rhodospirillum rubrum* probed by T-S spectroscopy and singlet-triplet annihilation at low temperatures. *Photochem. Photobiol.* 57:19–23.

Van Stokkum, I. H. M., T. Scherer, A. M. Brouwer, and J. W. Verhoeven. 1994. Conformational dynamics of flexibility and semirigidly bridged electron donor-acceptor systems as revealed by spectrotemporal parametrization of fluorescence. *J. Phys. Chem.* 98:852–866.

Visschers, R. W., M. C. Chang, F. van Mourik, P. S. Parkes-Loach, B. A. Heller, P. Loach, and R. van Grondelle. 1991. Fluorescence polarization and low-temperature absorption spectroscopy of a subunit form of light-harvesting complex I from purple photosynthetic bacteria. *Biochemistry.* 30:2951–2960.

Visschers, R. W., R. Nunn, F. Calkoen, F. van Mourik, C. N. Hunter, D. W. Rice, and R. van Grondelle. 1993a. Spectrosopic characterization of B820 subunits from light-harvesting complex 1 of *Rhodospirillum rubrum* and *Rhodobacter sphaeroides* prepared with the detergent *n*-octyl-rac-2,3-dipropylsulfoxide. *Biochim. Biophys. Acta.* 1100:259–266.

Visschers, R. W., F. van Mourik, R. Monshouwer, and R. van Grondelle. 1993b. Inhomogeneous spectral broadening of the B820 subunit form of LH1. *Biochim. Biophys. Acta.* 1141:238–244.

Völker, S. 1989. Hole-burning spectroscopy. *Annu. Rev. Chem.* 40: 499–530.

Xiao, W., Lin, S., Taguchi, A. K. W., and N. Woodbury. 1994. Femtosecond pump-probe analysis of energy and electron transfer in photosynthetic membranes of *Rhodobacter capsulatus*. *Biochemistry.* 33: 8313–8322.